Non-Contact Electrical Conductivity Measurement Technique for Molten Metals

Won-Kyu Rhim and Takehiko Ishikawa*
Jet Propulsion Laboratory, California Institute of Technology,
4800 Oak Grove Drive, Pasadena, California 91109, USA

*On leave from the National Space Development Agency of Japan

ABSTRACT

A non-contact technique of measuring the electrical conductivity (or resistivity) of conducting liquids while they are levitated by the high temperature electrostatic levitator in a high vacuum is reported. This technique, which utilizes the principle of asynchronous induction motor, measures the relative changes in torque by applying a rotating magnetic field to the sample. Changes in electrical resistivity was related to the measured torque using the formula developed for induction motor. Validity of this technique was demonstrated using a pure aluminum sample around its melting temperature. When the measurement results are calibrated at a literature value of resistivity at the melting point, our resistivity data around the melting point can be expressed by

$r_{e,liq} = 24.19 + 1.306 \times 10^{-2} (T - T_m)$ $\mu\Omega$·cm over $T_m \sim 1160$ K,

$r_{e,solid} = 10.77 + 1.421 \times 10^{-2} (T - T_m)$ $\mu\Omega$·cm over 700 K ~ T_m,

and the thermal conductivity as determined by the Wiedemann-Franz-Lorenz relation from these resistivity data are given by

$\kappa_{liq}(T) = 94.61 + 4.41 \times 10^{-2} (T - T_m)$ $W\,m^{-1}\,K^{-1}$,

$\kappa_{solid}(T) = 211.13 - 7.57 \times 10^{-2} (T - T_m)$ $W\,m^{-1}\,K^{-1}$.

Both electrical and thermal conductivities are in close agreement with the literature, confirming the validity of the present technique.

1. Introduction

Electrical conductivity is one of the most sensitive indicators of changes in the nature of the chemical binding. In general, the electrical conductivity is proportional to the carrier density and the carrier mobility. A change in the nature of chemical binding primarily alters the carrier density, and the structural changes alter the carrier mobility. The very early investigation of metals showed that the conductivity decreases approximately by a factor 2 at a melting point, while it increase in silicon and germanium as they transform from semiconducting solids to conducting. Electrical resistivity plays important roles in technical applications: it controls flow of melts under the influence of electromagnetic force in the process of refining or growing semiconductor crystals, and it is a sensitive measure of concentration fluctuation in a critically mixed liquid alloys near critical point in the homogeneous liquid phase.

In a conventional rotating magnetic field method for electrical conductivity, a cylindrical container holding a molten liquid is suspended by a tungsten wire, and the torque experienced by the hanging cylinder is measured when a rotating magnetic field is applied[1]. However, chemically reactive liquids, especially molten refractory materials, contained in the cylinder may be easily contaminated altering intrinsic electrical properties. Furthermore, one cannot expect those liquids to reach deeply undercooled state as long as container provides heterogeneous nucleants which trigger early solid phase nucleations.

In this paper we present a non-contact electrical conductivity measurement technique which was developed for the high temperature electrostatic levitator(HTESL)[2]. Non-contact processing of refractory materials using the HTESL will allow us to investigate properties of molten liquids without contamination both in their superheated as well as undercooled liquid states. Since a melt in the HTESL is well isolated from container walls through high vacuum, the melt will maintain its intrinsic properties, and it will also provide a rare situation of investigating structure and properties of deeply undercooled liquid state.

Also demonstrated in this paper is the determination of thermal conductivity of aluminum using the measured electrical conductivity data. Accurate measurement of thermal conductivity of molten metals is usually more difficult than the measurement of electrical conductivity. Inaccuracy is primarily caused by various flows taking place in a melt. Flows resulting from density difference in the presence of gravity, and Marangoni flow caused by non-uniform surface tension might be two powerful examples. However, if thermal and electric conductions take place primarily by free electrons, these two conductivities are connected through the Wiedemann-Franz-Lorenz law. Use of this law may allow us to obtain more accurate values for thermal conductivity from accurately measured electrical conductivity.

2. Experimental Apparatus and Approach

The High Temperature Electrostatic Levitator (HTESL) levitates a sample 1 to 3 mm in diameter between a pair of parallel disk electrodes spaced about 12 mm apart (Fig. 1). The electric field between these two electrodes generates an electrostatic force on a charged sample to cancel the gravitational force, and the four small side electrodes around the bottom electrode control the sample position along horizontal direction. The four coils positioned around the top electrode produce horizontal magnetic field which rotates at a appropriate frequency in order to induce sample rotation around vertical axis. The electrode assembly is housed by a stainless steel chamber which is typically evacuated to 10^{-8} Torr before sample heating begins. Samples are heated using a 1-kW xenon arc lamp. Detailed description of the HTESL is given in an earlier publication [2].

Four identical coils were wound. Each coil was wound on a glass spool (28 mm in length, and ~ 8 mm in diameter) with 28 gauge insulated copper wire. Spools were made out of silica glass for electrical insulation purpose since the coils were to be mounted in the close proximity of the high voltage electrode (the top electrode). When 400 turns were wound on each spool, each coil showed ~ 34 mH and ~ 5.3 ohm. When a soft iron core (0.25 inch in diameter, and 2.25 inches in length) was slid through each coil, approximately 3.2 mili-Tesler of magnetic filed could be produced at an end of the core when the coil carried 140 mA. As shown in Fig. 1, these four coils were mounted on the top electrode with iron cores deeply imbedded in it to maximize the magnetic field experienced by a levitated sample. Installing the coils on the top electrode, although it involved less than trivial high voltage insulation problem, was chosen since the space below the bottom electrode was occupied by the sample catcher and the sample storage/retrieval carousel.

The four coil assembly so mounted were driven by a current producing electronic assembly as shown in Fig. 2. A dual channel signal generator (HP 3326A) produce two low level sinusoidal signals with 90 degrees phase difference. We found that 400 Hz was adequate frequency for the present experiment. These two signals were then amplified by two separate amplifiers (HP 6825A) before they were connected to a switch box. This switch box does the traffic control of currents which are going through each coils to produce various magnetic fields. This switch has the following four settings: (i) an OFF switch cuts off all currents through the coils, (ii) a CLOCKWISE switch wires the coils so that the horizontal magnetic field seen by the sample rotates in the clockwise direction, (iii) a C-CLOCKWISE reverses the field rotation from clockwise, and (iv) an additional switch not shown in Fig. 2 is a VERTICAL switch which connects the coils in such a way to produce magnetic field along vertical direction at sample position. This VERTICAL switch is built-in so that it can damp sample rotation if its rotational axis is other than vertical direction. The CLOCKWISE or the C-

CLOCKWISE modes can be used either to accelerate or decelerate the sample depending upon its current rotational state. The currents flowing through each set of coils are monitored by measuring voltages across a 1 ohm resistor.

Accurate measurements of sample rotation frequency is important for accurate determination of torque imparted to the sample at different instantaneous rotation frequency. In the present experiment, a He-Ne laser beam was directed to the sample and the reflected beam was detected by a silicon photo-detector. The output voltage of the detector was amplified and digitized to get the Fourier power spectrum using a micro-computer. Such power spectrum showed peaks at all harmonics of the sample rotation frequency. An additional method which was used in parallel with the spectrum method was to utilize the strobe effect created by TV monitor. Regular monitors run at the 30 Hz frame rate (or at the 60 Hz field rate). A CCD camera running at a fast shutter speed was mounted on a tele-microscope to produce a magnified sample image on a TV screen. Whenever the sample rotation rate approaches one of the harmonic or sub harmonic frequencies of the 60 Hz field rate, the sample seems to slow down to show a completely static image at the harmonic/sub-harmonic frequency. Identification of 15, 20, 30, 40, or 60 Hz of sample rotation rate could be done precisely (within 0.01 Hz). Such a stroboscopic approach assisted by the power spectrum display allowed unambiguous determination of sample rotation frequency. When the drop shape is axi-symmetric, the methods described above can be applied only when there are some distinguishable surface structure on the drop. On the surface of the molten aluminum drop used in the present experiment, several aluminum oxides patches floating on the drop surface served as indicators.

3. Experimental Procedure and Results.

The basic principle of the present sample rotation mechanism is essentially the same as the asynchronous induction motor. The four coil assembly works as the stator while the levitated sample acting as the rotor. According to the principle of induction motor[3, 4], if an ac voltage E_1 at frequency ω_s is applied to a stator having resistance R_1 and inductance L_1, the torque τ experienced by the rotor (having its own resistance R_2 and inductance L_2) which is rotating at an instantaneous frequency ω is given by

$$\tau = \frac{\omega_s E_1^2}{R_1^2 + \omega_s^2 L_1^2}\left(\frac{sR_2}{R_2^2 + s^2 L_2^2}\right), \tag{1}$$

where

$$s \equiv \frac{\omega_s - \omega}{\omega_s}. \tag{2}$$

It is clear from Eq. (3) that, in order to measure the resistivity of a rotor, it is important to keep E_1 and ω_s constant throughout the measurement process. In this experiment, this requirement was satisfied by maintaining the stator currents constant. The Eq. (1) was put on a test by levitating an aluminum sphere, and measuring torque as a function of instantaneous sample rotation frequency. It can be seen in Fig. 3 that at a fixed stator current, the torque is linear function of the instantaneous sample rotational frequency. This means that the relationship $R_2^2 >> s^2L^2$ is well satisfied in Eq. (1), transforming the equation to a simpler form:

$$\tau = \left(\frac{\omega_s E_1^2}{R_1^2 + \omega_s^2 L_1^2}\right)\frac{1}{R_2}\left(1 - \frac{\omega}{\omega_s}\right). \qquad (3)$$

This equation shows that, when the left parenthesis (the stator term) is kept constant, the measured torque decreases linearly as a function of the rotor frequency and its gradient is inversely proportional to the resistance of the rotor. Fig. 3 shows the results obtained at three different coil (stator) currents. If the stator current is kept constant, any changes in the slope of this line must be related to changes in electric resistance of rotor. In the absence of any ferromagnetic materials (those soft iron cores in the present case), the measured torque should be proportional to the square of the current. As can be seen in this figure, the proportionality between the torque and the square of the coil current holds only approximately. However, it is worth emphasizing that the present technique relies heavily on the linear relationship between the torque and the instantaneous rotor frequency when the stator term is fixed.

Once the validity of Eq. (3) was demonstrated using a solid aluminum sphere, we are ready to apply it on a molten material whose resistivity around its melting temperature is well known. A pure aluminum was chosen for such a material. The sample material was heated above its melting point while it is levitated in the HTESL. For reasons of accurate detection of the sample rotation frequency, the average torque of the drop rotation frequencies between 15 Hz and 30 Hz, and back to 20 Hz was measured by timing each interval, instead of measuring the torque on the sample in the neighborhood of $\omega = 0$. This is justified as long the linearity between torque and rotational frequency holds as shown in Fig. 3. According to Eq. (3), when the frequency of applied rotating field is 400 Hz, the wind-up torque is given by

$$\tau_+ = \frac{C}{R_2}\left(1 - \frac{25}{400}\right), \qquad (4)$$

and the wind-down torque is given by

$$\tau_- = \frac{C}{R_2}(1+\frac{25}{400}),, \tag{5}$$

giving the average torque to be

$$\bar{\tau} = \frac{\tau_+ + \tau_-}{2} = \frac{C}{R_2}, \tag{6}$$

which is identical to the torque measured at 0 Hz. In the above equations, C represents the stator term shown in Eq. (1). Since the average torque exerted on a sample which changed its rotation frequency from ω_1 to ω_2 between the time t_1 and t_2 can be expressed by

$$\bar{\tau} = \frac{I(\omega_2 - \omega_1)}{t_2 - t_1} = I\frac{\Delta\omega}{\Delta t}, \tag{7}$$

in which I being the moment of inertia of the sample, a comparison with Eq. (6) shows that R_2 should be proportional to Δt if $I\Delta\omega$ remains constant. Indeed $\Delta\omega$ can remain fixed (at 10 Hz for example in the present experiment). If we express with $(\Delta t)_+$ the time interval measured as the molten aluminum drop was spun from 20 Hz to 30 Hz, and with $(\Delta t)_-$ the time taken from 30 Hz back to 20 Hz, the average torque can be expressed by

$$\bar{\tau} = \frac{\tau_+ + \tau_-}{2} = I\Delta\omega\frac{(\Delta t)_+ + (\Delta t)_-}{(\Delta t)_+(\Delta t)_-}. \tag{8}$$

If we compare Eq. (6) with Eq. (10), at a fixed $I\Delta\omega$, R_2 should be proportional to the measured time intervals by

$$R_2 = \frac{C}{I\Delta\omega}\frac{(\Delta t)_+(\Delta t)_-}{(\Delta t)_+ + (\Delta t)_-}. \tag{9}$$

Such time interval measurements were repeated at many different sample temperature both above and below the melting point. Also recorded at each temperature was the drop images (at the 20 Hz and 30 Hz) which were used to calibrate the final resistivity results due to changing moment of inertia. (The moment of inertia showed slight change as the sample shape changed at different rotation frequency and sample temperature (see Fig. 4). Final torque took into account such changes in moment of inertia.) When the time interval data so obtained by Eq. (9) around the melting temperature (T_m = 933.452 K) was calibrated by the resistivity of molten aluminum at the melting point (24.185 $\mu\Omega$·cm) given by a reference value[1], the resistivity data obtained at different temperature are as shown in Fig. 5. The solid lines are the linear fits to the data for the solid and the liquid branches which can be expressed by

$$r_{e,liq} = 24.19 + 1.306 \times 10^{-2} (T - T_m) \quad \mu\Omega\cdot cm, \tag{10}$$

while the expression by Iida et al. is given by

$$r_{e,liq} = 24.185 + 1.45 \times 10^{-2} (T - T_m) \quad \mu\Omega\cdot cm. \tag{11}$$

Since Iida's resistivity value at $T = T_m = 933.452$ K was used as the reference point the first terms in each expression should be identical. However, our temperature dependence of resistivity, $r_{e,liq}/dT$, is approximately 10 % smaller than that of Iida's. For the resistivity of solid phase at T_m, our result can be expressed by

$$r_{e,solid} = 10.77 + 1.421 \times 10^{-2} (T - T_m) \quad \mu\Omega\cdot cm. \tag{12}$$

Only literature data we could find on the resistivity of solid aluminum near melting point was $r_{e,solid}(T_m) = 10.9$ [1] which is in close agreement with our result. It is worth noting that $r_{e,solid}/dT$ we obtained near T_m is substantially different from that of the room temperature value, 0.429×10^{-2} $\mu\Omega\cdot cm/K$, given in the literature[5].

Since both solid and molten aluminum are conductors where free electrons are responsible for the electrical and thermal conductivities, one can use the Wiedemann-Franz-Lorenz law to relate the thermal conductivity with the electric resistivity:

$$\frac{\kappa_{liq} r_{liq}}{T} = \frac{\pi^2 k^2}{3e^2} \equiv L_o = 2.45 \times 10^{-8} \quad W\Omega K^{-2}, \tag{13}$$

where k is the Boltzman constant and e is the electron charge. The constant $L_o = \pi^2 k^2 / 3e^2$ is the Lorenz number whose validity was experimentally confirmed with high accuracy by Busch et al.[6].

Using the Eq.s (12), (14) and (15), one can obtain the following expressions for the thermal conductivities of solid and molten aluminum:

$$\kappa_{liq}(T) = 94.61 + 4.41 \times 10^{-2} (T - T_m) \quad W\,m^{-1}\,K^{-1} \quad \text{over } T_m \sim 1160 \text{ K}, \tag{14}$$

$$\kappa_{solid}(T) = 211.13 - 7.57 \times 10^{-2} (T - T_m) \quad W\,m^{-1}\,K^{-1} \quad \text{over } 700 \text{ K} \sim T_m. \tag{15}$$

These results are shown in Fig. 6 along with several other values from the literature[7-10]. The agreement between our result with independently measured thermal conductors from the literature are quite good.

4. Discussions

In this paper we described a non-contact technique which measures the electrical conductivity of molten metals. This is probably the first attempt of its kinds which can be applied to levitated melts. Having adapted to work on a melt levitated by HTESL in a high vacuum, it may be applicable to measure electrical conductivity of highly reactive melts of refractory materials as well as deeply undercooled melts of glass forming materials. This technique measures relative changes in electrical conductivity for a given levitated sample as a function of temperature. Therefore, it requires a reference data for calibration. For liquids where such reference data are not available, this technique may be extended in the future to a carefully selected standard sample for calibration.

Wiedemann-Franz-Lorenz law was used to determine the thermal conductivity of solid and liquid aluminum showing good agreement with independently measured reference value. Such indirect measurement of thermal conductivity may be proved to be important particularly for low viscosity liquids where direct measurement of thermal conductivity is susceptible to errors caused by the convective flows within the liquids.

As an application of the present technique, direct measurement of electrical conductivity and indirect determination of thermal conductivity through the Wiedemann-Franz-Lorenz law were carried out on a molten germanium with good results. These will be published elsewhere[11].

Acknowledgments:

The authors would like to thank Mr. Daniel Barber and Dr. Paul-Francois Paradis for various assistance in this work. This work was carried out at the Jet Propulsion Laboratory, California Institute of Technology, under contract with the National Aeronautical and Space Administration.

References:

(1) T. Iida and R. I. L. Guthrie, The Physical Properties of Liquid Metals (Clarendon press, Oxford, 1988), p. 228.

(2) W. K. Rhim, S. K. Chung, D. Barber, K. F. Man, G. Gutt, A. Rulison, and R. E. Spjut, Rev. Sci. Instrum. 64: 2961 (1993).
(3) S. A. Nasar and I. Boldea, Electric Machines (Steady tate Operation), Hemisphere Publishing Corporation 1990
(4) P. L. Alger, Nature of Induction Machine, Gordon and Breach Science Publishers 1965
(5) HandbooK of Chemistry and Physics 72nd, CRC Press, Ed. D. R. Lide.
(6) G. Busch, H. -J. Guntherodt, W. Haller, and P. Wyssmann, Phys. Lett. 43A, 225, 1973
(7) K. C. Mills, B. J. Monaghan, and B. J. Keene, "Thermal conductivities of molten metals: Part 1 Pure metals", Int. Materials Rev. 41, 209, 1996
(8) S. D. Preston and K. C. Mills, High Temp.-High Press., to be published.
(9) Y. S. Touloukian, R. W. Powell, C. Y. Ho, and P. G. Klemens: Thermophysical Properties of Matter: Vol. 1 Thermal Conductivity of Metallic Elements and alloys, 1970, New York, IFI/Plenum Press.
(10) J. T. Schriempf, High Temp.-High Press., 4, 411-416, 1972
(11) W. K. Rhim and T. Ishikawa, "Thermophysical Properties of Molten Germanium Measured by the High Temperature Electrostatic Levitator", (Submitted to J. Crystal Growth, 1998)

Figure Captions:

Fig. 1. Top and side views of the electrode assembly with rotation coils designed for the High Temperature Electrostatic Levitator at JPL. A charged conducting sample levitated between the electrodes can be rotated around vertical direction when a rotating magnetic field is applied around the same direction.

Fig.2. A schematic diagram of an electronics assembly which generates and channels appropriate electric currents to the coils to produced desired magnetic field at the sample position.

Fig. 3. Linear relationship between the measured torque on a levitated aluminum sphere (2.38 mm in diameter) and its instantaneous rotation frequency for three different values of coil current. The rotation frequency of applied magnetic field was 400 Hz.

Fig. 4. Side views of a levitated aluminum drop showing spherical shape when it is static (top picture), and oblate spheroid when it is rotating at the rate of at 60 Hz around vertical axis (bottom picture).

Fig. 5. Electrical resistivity of a pure aluminum measured as a function of temperature using the present technique. The literature value of resistivity of molten aluminum at the melting temperature was used as a single calibration point to obtain this result.

Fig. 6. Thermal conductivity of molten aluminum obtained from the results shown in Fig. 5 using Wiedemann-Franz-Lorenz law, and other values in the literature for comparison purpose.

Top view

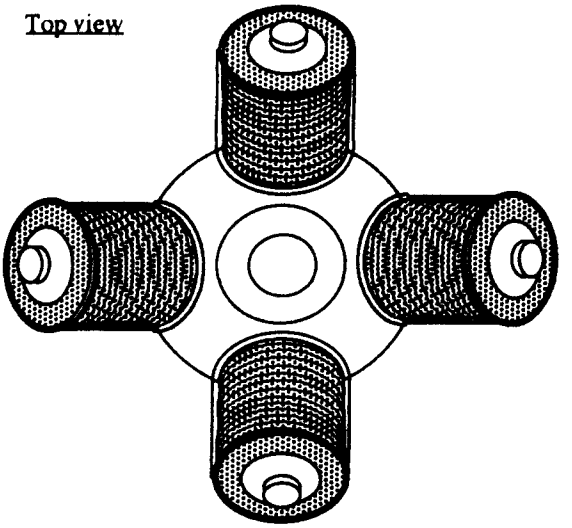

Side View

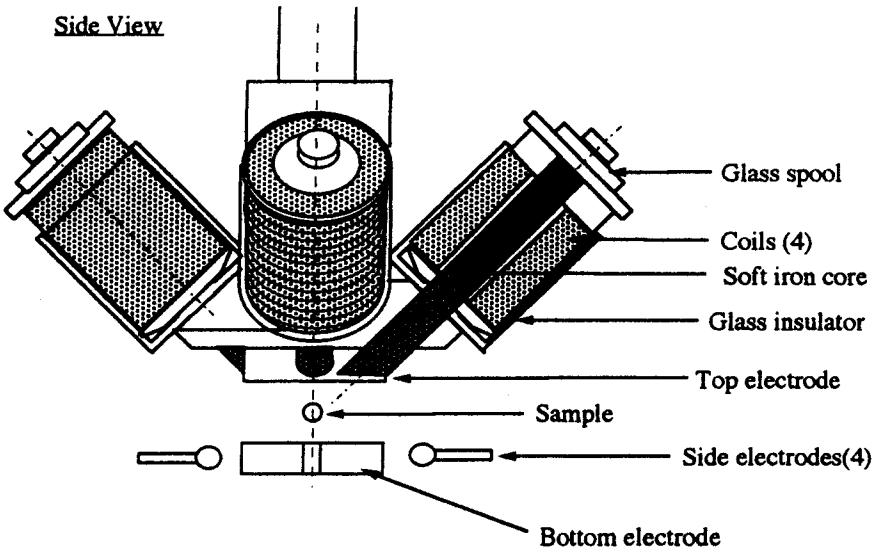

Fig 1

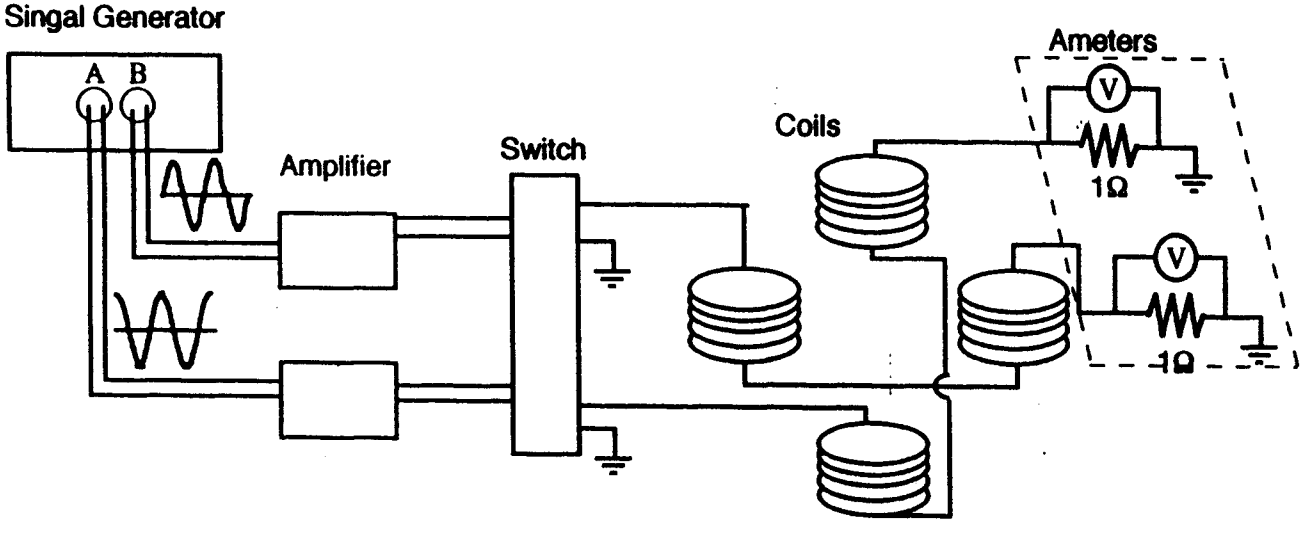
Singal Generator
A
B
Amplifier
Switch
Coils
Ameters
V
1Ω
V
1Ω

Fig 2

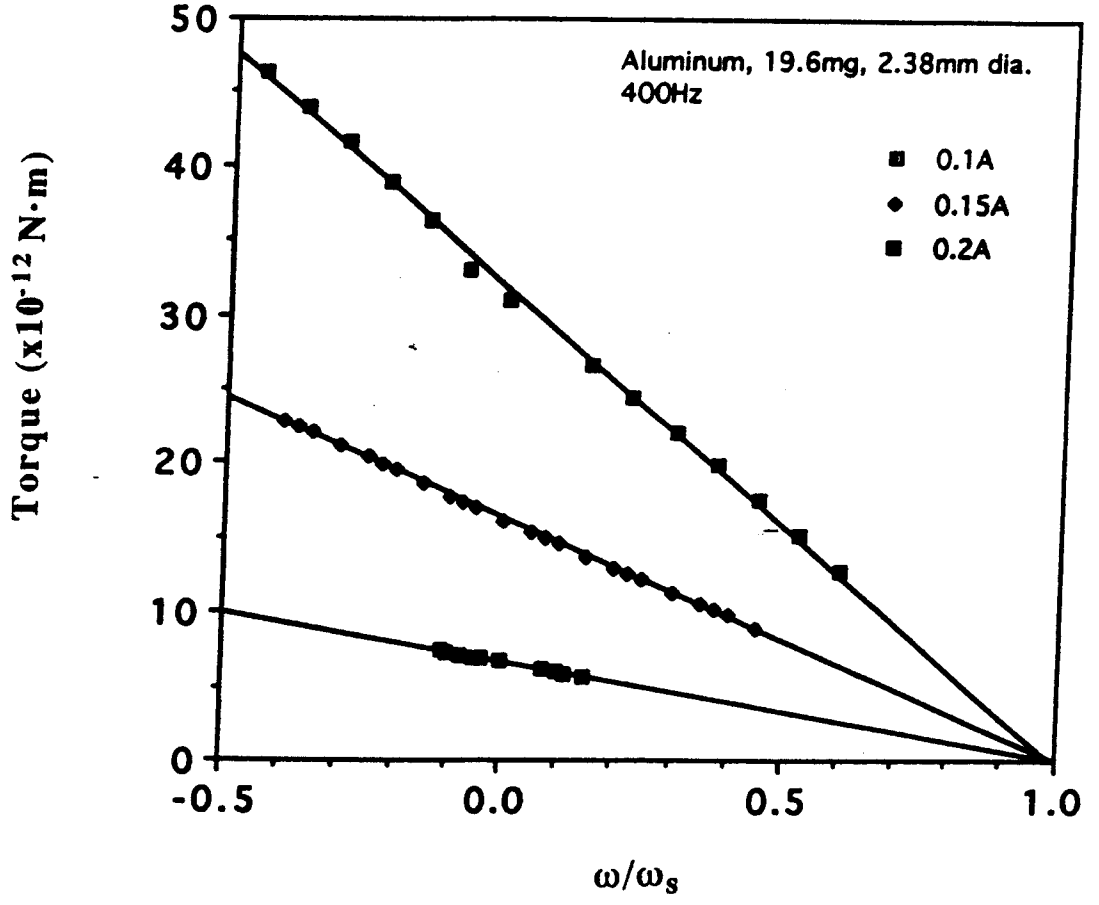
Aluminum, 19.6mg, 2.38mm dia.
400Hz
0.1A
0.15A
0.2A
Torque (x10⁻¹² N·m)
50
40
30
20
10
0
-0.5
0.0
0.5
1.0
ω/ωs

Fig 3

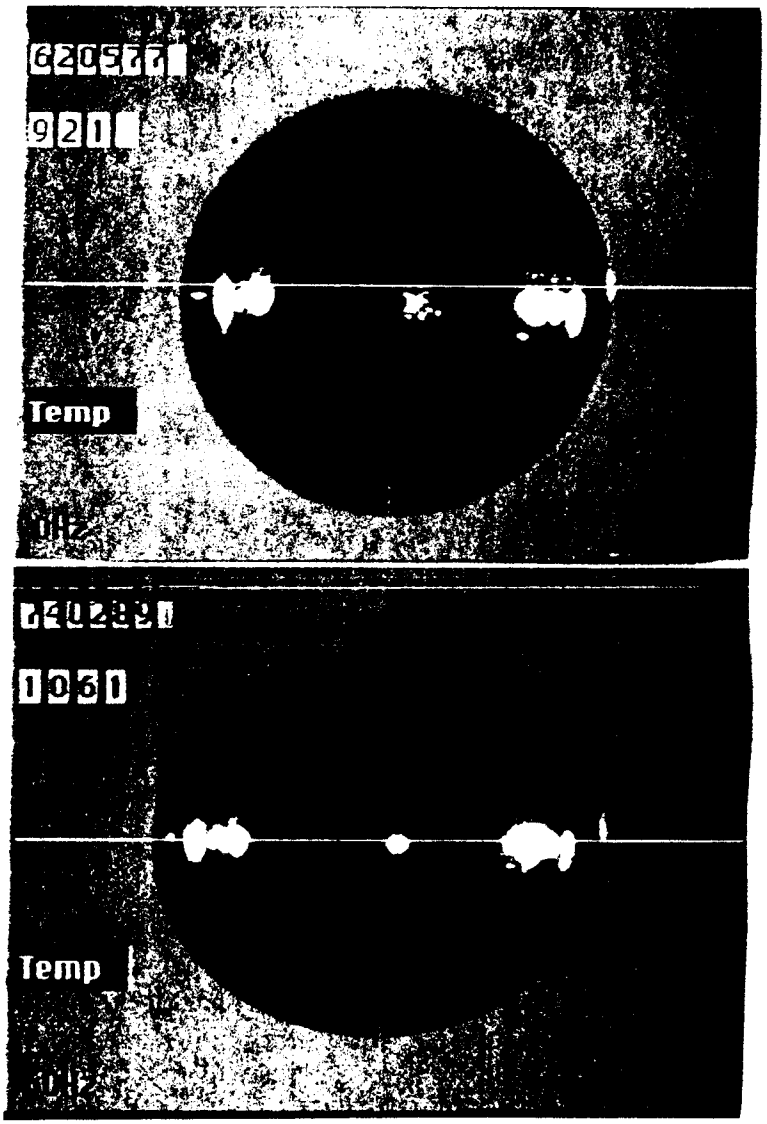

Fig 8

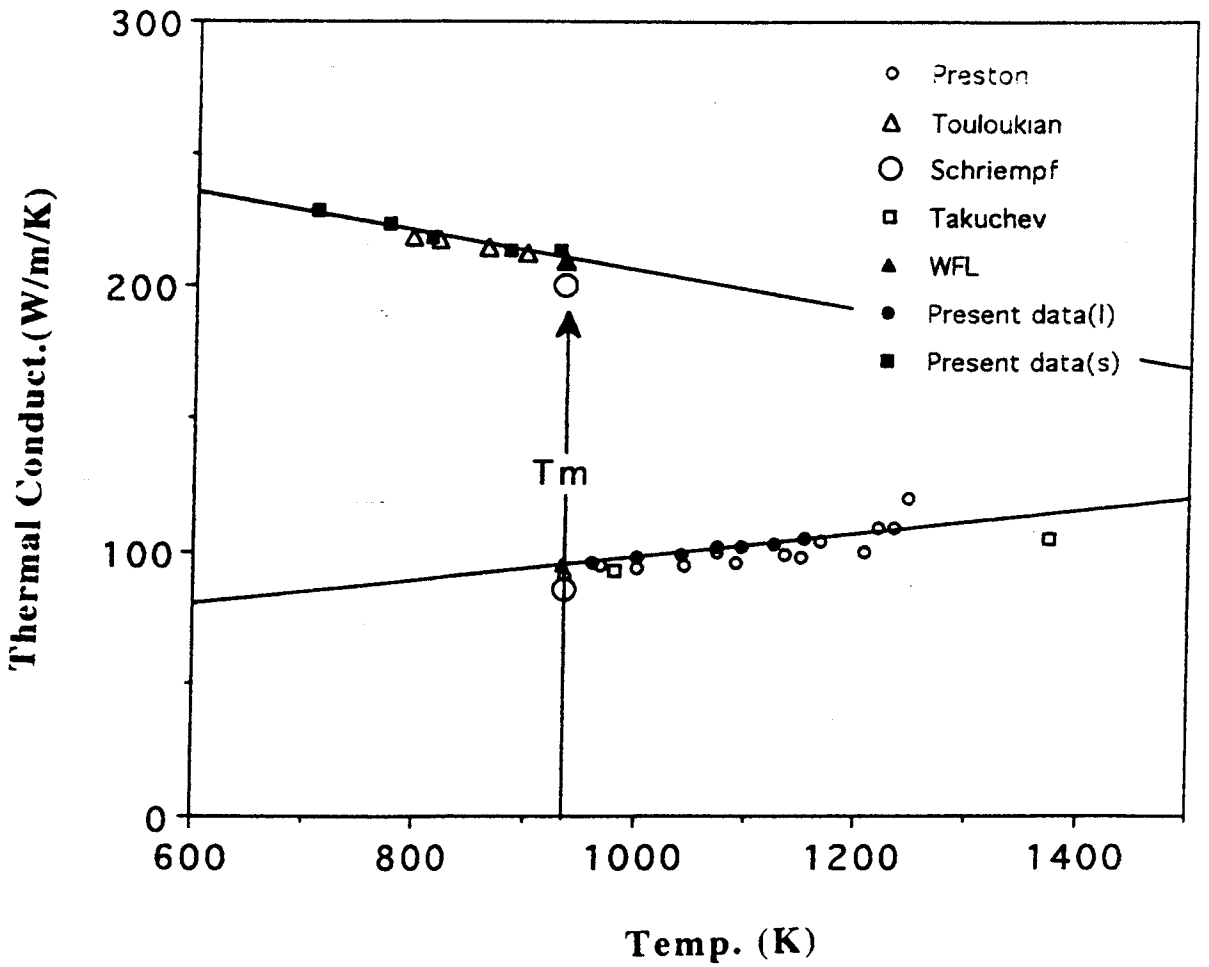
300
200
100
0
600
800
1000
1200
1400
Thermal Conduct.(W/m/K)
Temp. (K)
Tm
Preston
Touloukian
Schriempf
Takuchev
WFL
Present data(l)
Present data(s)

Fig 5

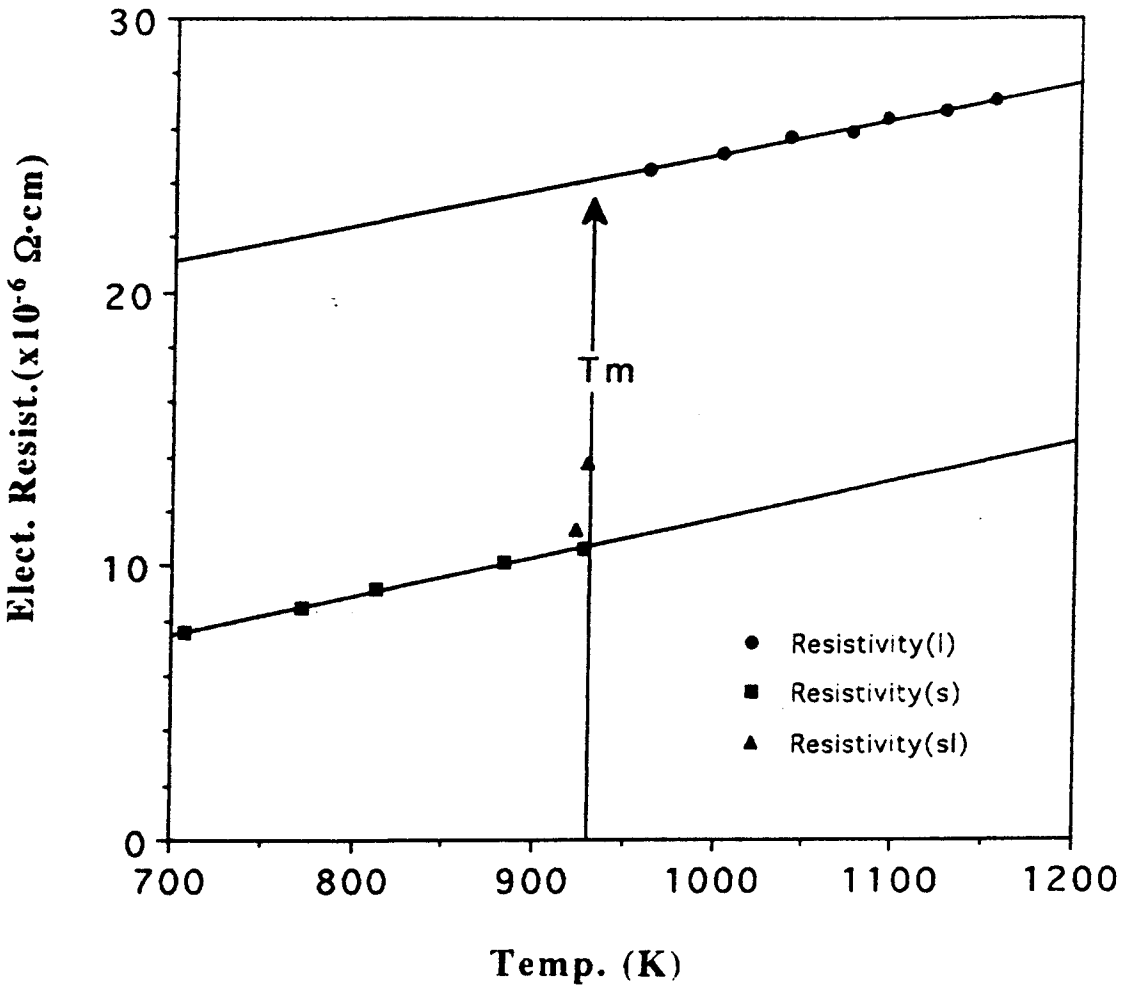
30
20
10
0
700
800
900
1000
1100
1200
Elect. Resist.(x10⁻⁶ Ω·cm)
Temp. (K)
Tm
Resistivity(l)
Resistivity(s)
Resistivity(sl)

Fig 6